Paleobiology, 49(3), 2023, pp. 454–470
DOI: 10.1017/pab.2022.48

PALEOBIOLOGY
A PUBLICATION OF THE Paleontological SOCIETY

Article

Convergent evolution of spherical shells in Miocene planktonic foraminifera documents the parallel emergence of a complex character in response to environmental forcing

*Peter Kiss**, *Natália Hudáčková*, *Jürgen Titschack*, *Michael G. R. Siccha*, *Zuzana Heřmanová*, *Lóránd Silye*, *Andrej Ruman*, *Samuel Rybár*, *and Michal Kučera*

Abstract.—The spherical encompassing final chamber of the planktonic foraminifera *Orbulina universa* is a prime example of a complex character whose evolution has been documented by a sequence of intermediate forms. However, the mechanism that induced evolution of the spherical chamber remain unclear. Here we show that shortly after the emergence of *Orbulina*, documented throughout the oceans, a convergent evolutionary transition occurred in the semi-isolated Paratethys, leading to the emergence of the endemic *Velapertina*, which occupied a similar niche to *Orbulina* in the surface waters. Using X-ray computed tomography scanning, we show that the evolution of the encompassing final chamber involved the same sequence of steps in both lineages, combining a progressively spherical shell shape with changes in the position, number, and sizes of apertures. The similarity in the sequence of character acquisitions suggests structural determinism in the way foraminiferal shells are constructed and the presence of natural selection favoring a spherical morphology. Collectively, the emergence of spherical chambers in the two lineages at a similar time suggests that the evolution of this spectacular complex character occurred in response to a singular environmental driver.

Peter Kiss. MARUM—Center for Marine Environmental Sciences, University of Bremen, Leobener Strasse 8, D-28359 Bremen, Germany; Department of Geology and Paleontology, Faculty of Natural Sciences, Comenius University in Bratislava, Mlynská dolina, Ilkovičova 6, 842 15 Bratislava, Slovakia. E-mail: peter.kiss03@gmail.com, kiss56@uniba.sk

Natália Hudáčková, Andrej Ruman, and Samuel Rybár. Department of Geology and Paleontology, Faculty of Natural Sciences, Comenius University in Bratislava, Mlynská dolina, Ilkovičova 6, 842 15 Bratislava, Slovakia. E-mail: natalia.hudackova@uniba.sk, winchestersk@yahoo.com, samuelrybar3@gmail.com

Jürgen Titschack‡. Senckenberg am Meer, Marine Research Department, D-26382 Wilhelmshaven, Germany.
‡Present address: MARUM—Center for Marine Environmental Sciences, University of Bremen, Leobener Strasse 8, D-28359 Bremen, Germany. E-mail: jtitschack@marum.de

Michael G. R. Siccha and Michal Kučera. MARUM—Center for Marine Environmental Sciences, University of Bremen, Leobener Strasse 8, D-28359 Bremen, Germany. E-mail: msiccha@marum.de, mkucera@marum.de

Zuzana Heřmanová. National Museum, Prague, Václavské náměstí 1700/68, 110 00 Praha 1, Czech Republic. E-mail: zuzka.hermanova@gmail.com

Lóránd Silye. Department of Geology, Babeș-Bolyai University, Strada Kogălniceanu 1, 400084, Cluj-Napoca, Romania. E-mail: lorand.silye@ubbcluj.ro

Accepted: 16 December 2022
*Corresponding author.

Introduction

The evolution of complex characters has been contested since the first formulation of the theory of evolution by natural selection by Darwin (1859). In theory, the fossil record should allow direct assessment of the sequence of changes leading to the emergence of such traits, but because speciation may frequently occur in small, peripherally isolated populations that are rarely preserved but usually accompanied by rapid morphological change (Gould and Eldredge 1977, 1993; Kelley 1983; Spanbauer et al. 2018), the fossil record often lacks the necessary resolution. A notable exception is

0094-8373/23

the fossil record of marine plankton, such as planktonic foraminifera, which allows species' transformations to be traced through time and in space with unparalleled continuity (Malmgren et al. 1983; Coxall et al. 2007; Pearson and Ezard 2014; Bicknell et al. 2018).

An iconic example of gradual morphological transformation leading to the emergence of a complex character is the evolution of the spherical encompassing final chamber in the planktonic foraminifera *Orbulina universa* d'Orbigny, 1839, which is completely documented by a series of transitional forms leading from the ancestral *Trilobatus* (Spezzaferri et al. 2015) through the intermediate *Praeorbulina* (Olsson 1964) to the descendant *Orbulina* (Blow 1956; Jenkins 1968; Pearson et al. 1997). This transition occurred in the open ocean, and the transitional forms emerged throughout the cosmopolitan warm-water habitat of the evolving lineage within a very short time, providing several key biostratigraphic data (Kennett and Srinivasan 1983; Wade et al. 2011). The transition does not appear to be associated with a shift in the habitat of the evolving lineage (Pearson et al. 1997) and does not occur in association with any distinct global climatic event, making it difficult to speculate about the trigger for the emergence of the idiosyncratic shell form. However, a similar character evolved independently in an unrelated lineage of Paleogene foraminifera, culminating in the morphologically similar but substantially older *Orbulinoides* (Cordey 1968), implying that the spherical shape, minimizing the surface-to-volume ratio of the adult shell, may represent a response to a specific lifestyle or a morphological expression of a specific habitat among planktonic foraminifera.

Indeed, there is abundant morphological (Norris 1991), genetic (Weiner et al. 2015), and isotopic (Coxall et al. 2007) evidence for parallel or repeated evolution of specific chamber shapes and shell elements in planktonic foraminifera. Notable examples are the iterative evolution of compressed chambers with a keel (Norris 1991) or of digitate or radially elongated chambers (Coxall et al. 2007; Weiner et al. 2015). The prevalence of iterative evolution among planktonic foraminifera can be explained by the presence of strong constructional constraints, imposing functional limits on the geometric variability of shells constructed by sequential addition of interconnected chambers (Raup 1966). Alternatively, the repeated evolution of similar traits may reflect phenotypic integration, resulting from the existence of a developmental and genetic network controlling the emergence of morphological traits in an organism (Pigliucci 2003). Functional and developmental integration may be both heritable and interconnected, jointly shaping (or rather channeling) the phenotypic landscape of an evolving clade (Müller and Wagner 1996).

In the case of the emergence of the spherical shell shape in planktonic foraminifera, it appears that the Paleogene *Orbulinoides* (Decima and Bolli 1970) and the Neogene *Orbulina* (Blow 1956; Pearson et al. 1997) followed a similar sequence of steps during their evolution. However, it was only in *Orbulina* that the evolutionary trend culminated in the emergence of a complex character, involving at the same time the enlargement of the final chamber and the migration of the sutural apertures over the entire chamber surface in the form of areal apertures. This makes it difficult to speculate about the evolutionary mechanisms and potential drivers of the evolution of the complex character in *Orbulina*. However, next to these two well-known and globally distributed lineages, there also exists an additional case of the evolution of a spherical shell shape in planktonic foraminifera: the enigmatic *Velapertina*. The genus *Velapertina* is endemic to the Central Paratethys, where it appears to have repeated the same sequence of transitional steps as *Orbulina*, culminating in the acceleration of chamber growth rate combined with apertural displacements. The existence of a potential endemic form with shell morphology similar to the *Orbulina* lineage was first formally acknowledged by Łuczkowska (1955), who described these forms from the Miocene of the Carpathian Foredeep as *Globigerinoides indigena*. The independent origin of this lineage from the *Orbulina* lineage was highlighted by Popescu (1969), who assigned this species to a new genus, *Velapertina*. Popescu (1969) described two new species of the genus, but these appear to be extreme morphologies with aberrant (kummerform) final chambers and apertural bulla

https://doi.org/10.1017/pab.2022.48 Published online by Cambridge University Press

covering the sutural apertures, otherwise identical with *Velapertina indigena*. A fourth species, *Velapertina sphaerica* Popescu, 1987, has a morphology consistent with the *Orbulina* lineage. The origin of the idiosyncratic *Velapertina* remains unclear, but ever since its discovery, it has been reported only from Miocene deposits in the Paratethys.

Remarkably, the dating of the Miocene formations where the enigmatic *Velapertina* appears (NN6 Zone; e.g., Filipescu 1996; Hohenegger et al. 2014) implies that the evolution of the final encompassing chamber in this lineage took place very shortly after the emergence of *Orbulina* (NN4 Zone). This coincidence cast doubts on the nature of *Velapertina*, because there are only a few well-documented cases of endemic evolution in planktonic foraminifera (e.g., Rögl 1994; Darling et al. 2007; Aurahs et al. 2009; Huber et al. 2020), and because it proved difficult to establish by external morphology alone whether or not it represents a variant of *Orbulina* (Łuczkowska 1971; Szczechura 1984). Thus, the existence of *Velapertina* could so far not be used in arguments on evolutionary processes in planktonic foraminifera.

Here, we resolve the nature of *Velapertina* by revealing the interior shell architecture through X-ray computed tomography scanning of exceptionally well-preserved specimens and analysis of the full ontogenetic sequence from the first chamber (proloculus), through the juvenile, neanic, and adult stages (sensu Brummer et al. 1987), leading to the development of its final encompassing chamber during the terminal stage. We compare the ontogenetic trajectory of *Velapertina* with *Orbulina* and constrain the habitat of the taxa by stable isotopic investigation of the shells and discuss the evolutionary implications of the resulting findings.

Materials and Methods

In order to constrain the spatiotemporal distribution of *Velapertina* throughout the Paratethys and to resolve the degree of its co-occurrence with the *Orbulina* lineage, we carried out an extensive literature review, compiling all localities where either lineage has been reported (Fig. 1, Supplementary Table 1). Only localities that provide sufficient stratigraphic constraints to resolve the occurrences to the level of planktonic foraminifera Subzone M5b (*Praeorbulina glomerosa* Lowest-occurrence Subzone), Zone M5 (*Praeorbulina sicana* Lowest-occurrence Zone), Zone M6 (*Orbulina suturalis* Lowest-occurrence Zone), and Zone M7 (*Fohsella peripheroacuta* Lowest-occurrence Zone) were considered (Wade et al. 2011). The search was carried out by querying the literature through Google Scholar, using combinations of taxonomic (*Velapertina*, *Orbulina*, *Praeorbulina*, *indigena*, *suturalis*, *glomerosa*, *circularis*) and geographic (Paratethys) keywords. The taxonomy has been harmonized across the papers to the genus level, and in each case the occurrence and biozone has been recorded. In all cases where *Velapertina* was recorded as co-occurring with one of the other taxa, we made sure that the co-occurrence was reported from within the same sample in the sediment sequences described in each paper. Next to the canonical *Velapertina indigena* Łuczkowska, 1955, three more species of the genus have been formally described (Popescu 1969, 1973, 1987), but these have been so far only recorded from single localities, and in our opinion it remains questionable whether the described morphologies represent distinct taxa or extreme forms within a variable species.

The terminal-stage morphology is similar between the genera *Velapertina* and *Orbulina*, with the spherical encompassing final chamber having multiple small areal apertures (Fig. 2). Thus, we decided to study their relatedness by reconstructing the ontogenetic trajectory preserved in the sequence of chambers preceding the terminal spherical chamber. *Velapertina* is endemic to the Paratethys (Łuczkowska 1971) and can be studied only using material from this realm. Thus, to resolve the relatedness of *Velapertina* and *Orbulina*, we concentrated on specimens of the *Orbulina* lineage from the Paratethys, assuming that these are representative of populations that could be the nearest relatives of *Velapertina*. In addition, we have also analyzed one specimen of *Praeorbulina* from the Pacific, to ensure the morphology of the Paratethyan specimens is representative for the lineage at large. In the Paratethys, we concentrated on three localities (Fig. 1) of middle Miocene age (Badenian stage in the regional

https://doi.org/10.1017/pab.2022.48 Published online by Cambridge University Press

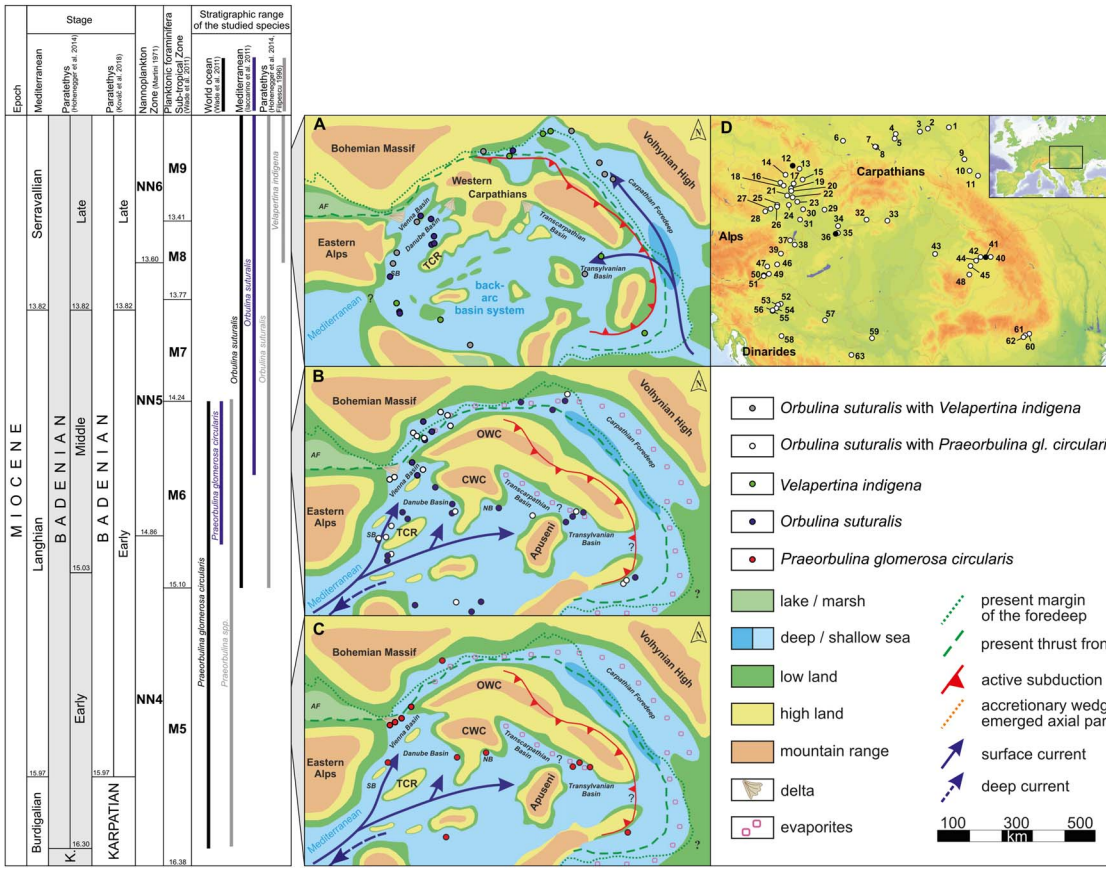

FIGURE 1. Serravallian (A) and Langhian (B, C) occurrences of *Velapertina indigena*, *Orbulina suturalis*, and *Praeorbulina glomerosa circularis* within the Central Paratethys. The Central Paratethys during the middle Miocene covered the Pannonian Basin system surrounded by the Alps, Carpathians, and Dinarides in central Europe (D). Data used for the compilation of species distribution (D) were collected from the literature, with numbers referring to the references listed in Supplementary Table 1. The known occurrences and co-occurrences of the discussed species are shown for each time interval. The synthesis reveals that *Velapertina* and the *Orbulina* lineage were widespread throughout the middle Miocene Central Paratethys and that the representatives of the two lineages had overlapping distributions with well-documented co-occurrences. Abbreviations: AF, Alpine Foredeep; CWC, Central Western Carpathians; OWC, Outer Western Carpathians; NB, Novohrad-Nógrád Basin; SB, Styrian Basin; TCR, Transdanubian High; ?, assumed short-lived seaway. Paleogeographic reconstructions of the Paratethys were taken from Kováč et al. (2017).

Paratethyan stratigraphy; Kováč et al. 2018), representing the time shortly after the origin of both lineages and exhibiting the best preservation of planktonic foraminifera, making it likely that the initial whorls inside the spherical shells of the studied species are preserved and suitable for X-ray computed tomography scanning and 3D rendering.

One well preserved *O. suturalis* specimen was obtained from a sample at 1303–1298 m in Modrany-1 well (47°50′58.5″N, 18°22′08.4″E, Locality 36 in Fig. 1) from the south-eastern part of the Danube Basin (Slovak Republic), dated to the Zone M6 or NN5 Zone (Vlček et al. 2020). At this site, *P. glomerosa circularis* was rare and did not yield specimens suitable for X-ray computed tomography scanning. Further material was collected from an outcrop of Badenian (Langhian) clays also assigned to Zone M6 or NN5 Zone at Jevíčko (49°38′15.6″N, 16°41′13.3″E, Locality 12 in Fig. 1) in Moravia (Czech Republic) (Reuss 1854; Bubík 2015). At this locality, one well-preserved specimen of *P. gl. circularis* and *O. suturalis* was taken for X-ray computed tomography scanning. The Pacific specimen of *P. gl. circularis* was selected from ODP Hole 872C, recovered in the vicinity of the Marshall Islands

https://doi.org/10.1017/pab.2022.48 Published online by Cambridge University Press

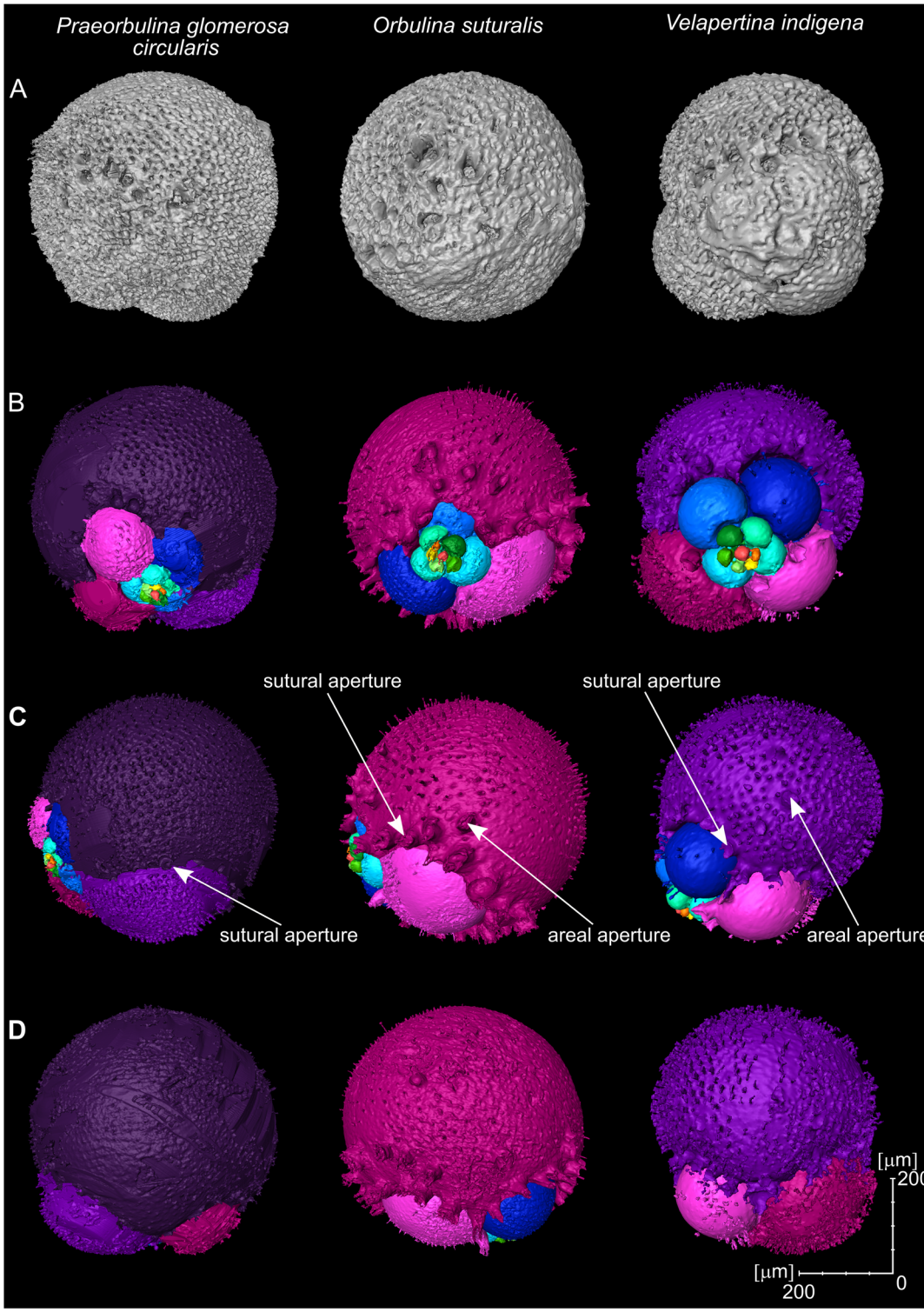

FIGURE 2. X-ray computed tomography scanning of shell architecture of representative specimens of *Praeorbulina glomerosa circularis*, *Orbulina suturalis*, and *Velapertina indigena* from the Central Paratethys. Species are shown from different perspectives: A, spiral view of external morphology; B, spiral view of internal morphology; C, side view of internal morphology; and D, umbilical view of internal morphology. It appears that the three species have similar external shell morphology with spherical shell shape and multiple apertures, but the X-ray computed tomography scanning data reveal distinct growth patterns of achieving the final encompassing chamber in *Orbulina* and *Velapertina* lineages.

https://doi.org/10.1017/pab.2022.48 Published online by Cambridge University Press

(Pacific Ocean). This sample is assignable to the middle Miocene Zone M5 or NN4 Zone, and the foraminifera were reported to be excellently preserved (Pearson 1995). Finally, well-preserved *V. indigena* specimens were retrieved from an outcrop at Chiuza (47°14′36.6″N, 24° 14′51.8″E, Locality 41 in Fig. 1), located in the northern part of the Transylvanian Basin (Romania), dated to the NN6 Zone, which corresponds to Zone M7–Zone M9 (*Fohsella fohsi* Taxon-range Zone; Filipescu 1996).

At localities Jevíčko and Chiuza and from the Modrany-1 core sample, about 200 g of sediment was collected. Samples were crushed into fragments of about 0.5 to 1 cm^3 size, soaked in tap water, diluted in 3% hydrogen peroxide (H_2O_2) until fully disintegrated, and wet sieved over 63 µm and 150 µm mesh sieves. The residues were then dried at 40°C for 24 hours and split. Planktonic foraminifera were manually picked and identified from the >150 µm size fractions. The sample treatment of material obtained from Hole 872C, leg 144, is given by Pearson (1995). Planktonic foraminifera taxonomy follows the concepts of Blow (1956), Łuczkowska (1971), and Pearson et al. (1997). Initially, 80 individuals of *O. suturalis* were isolated from the dried residue from Modrany-1, 80 individuals of *P. gl. circularis* and of *O. suturalis* from Jevíčko, 80 individuals of *P. gl. circularis* from the ODP Hole 872C sample, and 80 individuals of *V. indigena* from Chiuza. These specimens were subsequently transferred to a petri dish filled with water to separate out tests that were not filled with sediment. Specimens with sediment-filled chambers sank to the bottom of the petri dish, while those with empty shell interiors remained floating. From among the presumably unfilled tests, we selected two individuals per species (four individuals for the morphologically more variable *Velapertina*) with particularly good preservation and well-developed terminal-stage morphology for X-ray computed tomography scanning.

The X-ray computed tomography scanning was performed with the SkyScan 1172 high-resolution micro-computed tomography device at the Natural Museum in Prague (Czech Republic). Tube voltage was set to 40 kV, and the current source was 250 µA. No filter was used. Random movement was set to 5. Data were acquired with an angle slope of 0.2° and 180° rotation. The acquired data were processed using flat-field correction and reconstructed by the supplied software NRecon (Bruker), which resulted in an isotropic voxel size of 0.54 µm for the <0.5 mm large specimens. Each X-ray computed tomography scan was visualized and morphometrically analyzed with the software Amira ZIBE edition v. 2019.04 (Stalling et al. 2005; http://amira.zib.de). The shells were segmented into the sequential chambers, and any sediment remains within the chambers were manually removed with the *Segmentation editor*. The chambers were segmented by using the AmbientOcclusionField module and following the approach of Titschack et al. (2018) and Baum and Titschack (2016) (settings: number of rays: 156; ray length: ranging from 1 to 0.2 mm for every specimen and exceeding the cavity diameter in all other specimens). To separate the individual chambers within the shell, a DistanceMap of the intraspace was calculated as the basis for a CountourTreeSegmentation (persistence value: 0.05; see Titschack et al. 2018). The chamber separation was checked and manually corrected with the *Segmentation editor*. After this, the size extents (width, length, and height), volume, flatness, and elongation of the chambers, and the size extents (width, length, and height) and volume of the shell at different stages of growth were extracted with the ShapeAnalysis module, following Westin et al. (1997). The segmentation revealed that in all of the scanned specimens of *Orbulina* and *Praeorbulina*, and one of the *Velapertina* specimens, the full series of chambers was preserved and could be resolved. To characterize their coiling geometry, we extracted the centroids of all chambers in these specimens. In addition, we were also able to resolve the coiling geometry in *V. indigena* specimen 2, where the preservation allowed us to determine the total number of the chambers and to identify the starting point of their spiral. We used the chamber centroids to calculate the growth parameters introduced by Raup (1966) and Caromel et al. (2017): (1) translation rate of the whorl (T), (2) expansion rate of the whorl (W), (3) the generating curve with respect to the coiling axis modified by Caromel et al. (2017) (D), and (4) the

https://doi.org/10.1017/pab.2022.48 Published online by Cambridge University Press

distance between the chamber's centroid from the coiling axis in an *x,y* plane (R). For each specimen, we also recorded the total number of chambers and the number of whorls (#W) in the trochospire (Table 1).

We were able to characterize the pre-terminal morphology of all eight scanned specimens, including all four *Velapertina* specimens, where the earliest part of the chamber sequence of specimens 2, 3, and 4 was not preserved. Based on parameters extracted from only five chambers preceding the final chambers, we performed cluster analyses. In addition, by quantifying the shape of the chambers, the shape of the shell, the expansion rate of the chambers and the expansion rate of the shell for the five chambers before the final chamber (Table 1), we visualized the morphospace using nonmetric multidimensional scaling.

Exceptionally well-preserved specimens of planktonic foraminifera from Chiuza and Jevíčko were used for stable isotopic characterization of the habitat of the studied lineages. Despite a number of studies on the geochemistry of fossil planktonic foraminifera from the Central Paratethys (e.g., Báldi 2006; Kováčová et al. 2009; Scheiner et al. 2018), the only analysis including *Velapertina* is the study by Durakiewicz et al. (1997) (Locality 6 in Fig. 1). This study indicates a shallow habitat for *V. indigena*, overlapping with co-occurring *O. suturalis* and *Globigerinoides* sp., but the study has been conducted in an interval affected by the occurrence of evaporites (Durakiewicz et al. 1997), indicating that the oxygen isotopic composition of the local seawater may have been affected by isolation and evaporation, potentially biasing the oxygen isotopic results. Therefore, the stable isotopic habitat of the lineage relative to other planktonic foraminifera requires confirmation. The new measurements conducted here involved 15–20 specimens per species (approximately 100 µg), including individuals of *P. gl. circularis*, *Globigerina bulloides*, sinistrally and dextrally coiled *Neogloboquadrina* sp., and the benthic *Hansenisca soldanii* from Jevíčko, and *V. indigena*, *Globigerina bulloides*, *Globoturborotalita* sp., and *Globigerinoides* sp. from Chiuza. To account for the known size effect on stable isotopic composition of planktonic foraminifera (e.g., Ezard et al.

TABLE 1. Morphological variables used in the cluster analysis (variables marked with an asterisk symbol) and nonmetric multidimensional scaling (Fig. 4).

	Praeorbulina gl. circularis s. 1 (Paratethyan)	*Praeorbulina gl. circularis* s. 2 (ODP)	*Orbulina suturalis* s. 1	*Orbulina suturalis* s. 2	*Velapertina indigena* s. 1	*Velapertina indigena* s. 2	*Velapertina indigena* s. 3	*Velapertina indigena* s. 4
*Chamber-length growth rate [%]	32.60	33.97	33.35	37.09	35.83	34.00	39.23	25.04
*Chamber-width growth rate [%]	29.83	32.13	37.93	36.76	33.61	34.26	41.55	30.06
*Chamber- height growth rate [%]	26.58	21.62	37.18	21.90	34.60	34.29	47.71	35.60
Chamber length and shell length ratio	0.70	0.67	0.74	0.71	0.67	0.67	0.83	0.79
*Chamber elongation	0.84	0.86	0.77	0.81	0.88	0.87	0.73	0.84
*Chamber flatness	0.75	0.75	0.73	0.62	0.84	0.79	0.66	0.67
Chamber volume and shell volume ratio	0.55	0.51	0.56	0.56	0.54	0.57	0.67	0.54
Surface area and chamber volume ratio	0.12	0.12	0.12	0.14	0.12	0.11	0.17	0.11
*Shell length and height ratio	1.63	1.69	1.63	1.53	1.64	1.60	1.69	1.56
Shell length and width ratio	1.32	1.29	1.24	1.26	1.28	1.30	1.68	1.49
*Number of whorls [#W]	2.29	2.52	1.71	1.90	1.84	1.23	NA	NA
*Translation rate [T]	1.11	1.23	1.35	1.22	1.21	1.29	NA	NA
*Generating curve [D]	0.08	0.09	-0.02	0.06	0.10	0.00	NA	NA
*Expansion rate [W]	60.33	53.41	60.47	48.61	25.65	98.26	NA	NA
*Distance from the coiling axis [R]	143.88	138.94	105.34	96.95	48.53	126.19	NA	NA

https://doi.org/10.1017/pab.2022.48 Published online by Cambridge University Press

2015), individuals of *P. gl. circularis* were further divided into small (<200 μm) and large (>200 μm) specimens, while due to the observed large intraspecific shell size variability, small (<200 μm), moderate (200–300 μm), and large (>300μm) individuals were separated for *V. indigena*. The stable oxygen and carbon isotopic composition of the picked foraminifera were measured at MARUM, University of Bremen (Germany), with a Finnigan MAT 251 gas isotope ratio mass spectrometer connected to a Kiel 1 automated carbonate preparation device. The instrument was calibrated against the in-house standard (ground Solnhofen limestone), which in turn was calibrated against the NBS 19 standard reference material. Over the measurement period, the standard deviations of the in-house standard were 0.04‰ for $\delta^{13}C$ and 0.06‰ for $\delta^{18}O$. Data are reported in the delta-notation versus VPDB.

Results

Our synthesis of literature occurrences reveals that the *Orbulina* lineage and *Velapertina* lineage were widespread throughout the middle Miocene Central Paratethys (Fig. 1). Because most of the records derive from outcrops, which only cover a small part of the middle Miocene sedimentary record, it was not possible to reconstruct the temporal occurrence with a precision higher than foraminiferal Zone M5, Zone M6, and Zone M7 (Wade et al. 2011). At this resolution, the data synthesis indicates that *Praeorbulina gl. circularis* appeared in the Mediterranean region in the Langhian (Lirer et al. 2019), while the earliest representatives of *Praeorbulina* are recorded in the Paratethys during the Langhian (M5 or NN4 Zone, early Badenian stage), shortly after the global emergence of this lineage in the uppermost Burdigalian (Zone M5; Wade et al. 2011). During the Langhian (M6 or base of NN4 Zone), we document the first occurrence of *Orbulina suturalis* and the co-occurrence of *O. suturalis* with *P. gl. circularis* in a number of places throughout the Central Paratethys. This shows that this region displays a similar species succession in the evolving lineage, as seen in the Mediterranean (Lirer et al. 2019) and in the tropical world ocean (Wade et al. 2011).

Following the first appearance of *Orbulina*, *Velapertina indigena* evolved in the Central Paratethys in the Serravallian (M7 or NN6 Zone, late Badenian; Hohenegger et al. 2014; Kováč et al. 2018). We identified 17 Serravallian localities where *Velapertina* was found distributed throughout the Central Paratethys (Fig. 1). Of these, *Velapertina* co-occurred with *Orbulina* at 10 localities (co-occurrence implying the species were reported in the same sample), and there are only 9 localities, mainly in the Vienna Basin, where *Orbulina* has been reported but *Velapertina* has not. Within the stratigraphic resolution of our literature data synthesis, it is impossible to interpret whether the lack of *Velapertina* at some localities indicates an older age of those deposits. We can thus only conclude that at the given resolution of the Paratethyan stratigraphy, *Orbulina* and *Velapertina* had broadly overlapping distributions, with well-documented co-occurrences, but we cannot identify where in Paratethys *Velapertina* originated.

After establishing the biogeography and the pattern of co-occurrence of the two lineages in the Central Paratethys, we analyzed their shell geometry by X-ray computed tomography scanning. Five of the eight analyzed specimens showed well-preserved internal shell features with minimal sediment infill, allowing us to manually reconstruct the pattern of chamber addition from the proloculus. The *Praeorbulina* specimens had 15 and 16 chambers, the *Orbulina* specimens had 12 and 13 chambers, and one of the *Velapertina* specimens had 14 chambers (Figs. 2, 3). The initial whorl of the remaining *Velapertina* specimens proved to be damaged, with septae missing, and the shell architecture could therefore be reconstructed for specimen 2 only for the last 10 chambers and for specimens 3 and 4 for the last 8 chambers. The segmentation of the shell interior into the successive chambers reveals a pattern with rather constant and similar chamber growth rates throughout the ontogeny for all three taxa (Fig. 3A–C,E,F), with a conspicuous acceleration of growth rate for the final chamber occurring only in *Praeorbulina* and *Orbulina*. The average volume-based growth rate for the five successive chambers preceding the final chamber (forming an entire whorl and corresponding

https://doi.org/10.1017/pab.2022.48 Published online by Cambridge University Press

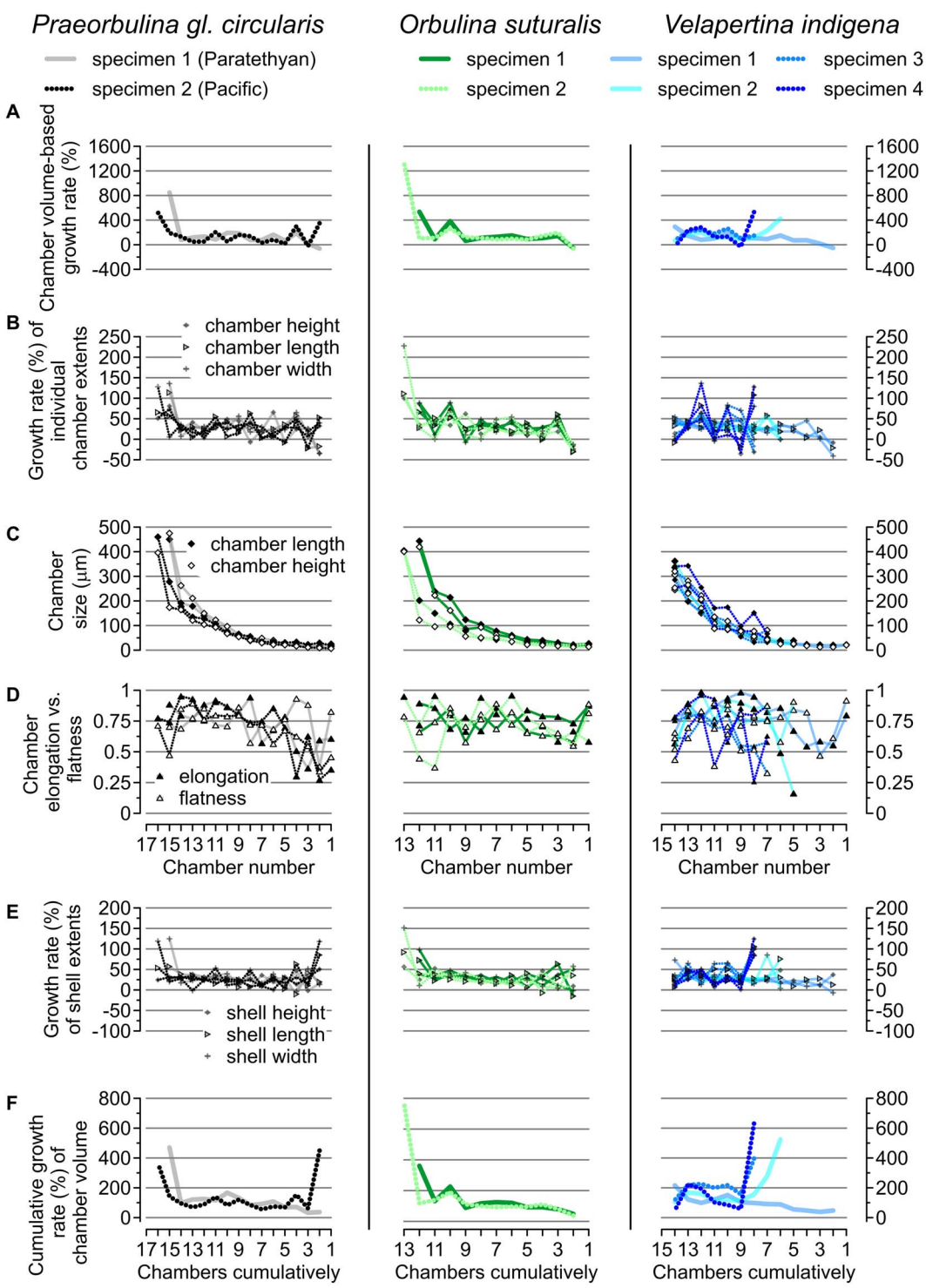

FIGURE 3. Ontogenetic trajectories of *Praeorbulina glomerosa circularis*, *Orbulina suturalis*, and *Velapertina indigena* extracted from the X-ray computed tomography scanning data. Different colors and lines denote different specimens. The growth trajectories of the analyzed species are plotted backward from the final chamber to the proloculus: A, growth rate based on the chamber volume; B, growth rate based on the chamber size extents (length, width, and height); C, chamber length and height ratio; D, chamber flatness and elongation ratio; E, cumulative growth rate based on chamber size extents (length, width, and height); F, cumulative growth rate based on chamber volume. For the two incompletely resolved specimens of *Velapertina*, we assumed for the purpose of data visualization that they also had 14 chambers, but values of chamber shape and size are only shown for chambers that could be fully resolved. The growth trajectories of the analyzed species are indeed similar; however, the shape of the final chamber and the lack of growth rate acceleration for the final ultimate chamber in *Velapertina* indicate a different growth pattern from the *Praeorbulina–Orbulina* lineage.

https://doi.org/10.1017/pab.2022.48 Published online by Cambridge University Press

to the adult stage; sensu Brummer et al. 1987) was in *Praeorbulina*, 122% and 126%; in *Orbulina*, 141% and 155%; and in *Velapertina*, 127%, 200%, 149%, and 139% (Fig. 3A). Whereas in *Praeorbulina* and *Orbulina*, the final chamber became more spherical (similar length and height; Fig. 3C,D), in *Velapertina*, the final chamber became conspicuously flatter, especially in specimens 2 and 4 (Fig. 3C,D).

The lack of growth acceleration toward the final chamber indicates that *Velapertina* must have achieved the spherical shell shape in a different manner than *Orbulina* and *Praeorbulina*. To assess the ontogenetic trajectory preceding the final chamber, we extracted the coordinates of the geometric centers of all chambers added before the final chamber and used these to describe the shape of the logarithmic spire. We used cluster analysis to visualize the similarity among the specimens. The outcome of this analysis shows higher similarity in the pre-adult ontogenetic trajectory and shell morphology between the two specimens of *Praeorbulina*, two specimens of *Orbulina*, and two specimens of *Velapertina*, indicating that the analysis likely captures a consistent aspect of the species' pre-adult shell architecture. Next, the analysis reveals that the analyzed shells of *P. gl. circularis* and *O. suturalis* follow a more similar ontogeny, whereas the two specimens of *V. indigena* are different (Fig. 4A). To account for the large morphological variability in *Velapertina*, also indicated by the larger distance between the two specimens seen in the cluster analysis of the spiral growth parameters (Fig. 4A), we carried out nonmetric multidimensional scaling to visualize the morphospace (Fig. 4B). The results confirm that *Velapertina* is more variable, but indicate that all four *Velapertina* specimens differ from *Praeorbulina* and *Orbulina*. Thus, both the analysis of the full ontogenetic trajectory (Fig. 4A) and the analysis of the five penultimate chambers (Fig. 4B) suggest that the similar adult shell shape with encompassing final chamber in *Velapertina* and in the *Orbulina* lineage conceals a morphologically different pre-adult ontogenetic trajectory.

After analyzing the shell architecture of the two lineages, we constrained the habitat of the lineages by comparing new stable isotopic analyses of their shells from Jevíčko and Chiuza with data from Durakiewicz et al. (1997). Our results at Jevíčko revealed a $\delta^{18}O$ offset of up to 1.5‰ between planktonic and benthic taxa. The benthic fauna at this site is represented by *Hansenisca soldanii*, which reveals the most positive (i.e., "coldest") $\delta^{18}O$ signature. Among the analyzed planktonic taxa, the specimens from the *Praeorbulina–Orbulina* and *Velapertina* lineages show more positive (i.e., "colder and thus deeper") $\delta^{18}O$ values, but these species have a greater enrichment of $\delta^{13}C$ as an indicator of the presence of symbionts (Birch et al. 2013; Fig. 5A). The Chiuza site, the best locality in terms of shell preservation of *V. indigena*, lacks benthic foraminifera, but the overlap in the $\delta^{18}O$ values among all of the analyzed planktonic species indicates that they likely all inhabited essentially the same surface layer. Here, we also found a conspicuous $\delta^{13}C$ enrichment in *V. indigena*, especially among the larger specimens, which is of a similar magnitude as in the co-occurring *Globigerinoides* sp. These results are congruent with the earlier study by Durakiewicz et al. (1997), who recorded a similar $\delta^{13}C$ enrichment in *V. indigena*, which is thus isotopically similar to *O. suturalis* and *Globigerinoides* sp. Nevertheless, those authors recorded overall more positive $\delta^{18}O$ values (Fig. 5B), which may reflect the more northerly location of their material or an isotopic enrichment due to evaporation, as evidenced by the presence of evaporites in their section. Collectively, these results indicate that *V. indigena* likely possessed symbionts, and its stable isotopic habitat cannot be distinguished from that of the *Orbulina* lineage.

Discussion

Even though the external shell morphologies of the *Orbulina* lineage and *Velapertina indigena* are similar (Fig. 2), with spherical shell shape and sutural and areal apertures, the X-ray computed tomography scanning data highlight a different internal shell architecture and a distinct growth pattern in *Velapertina* (Figs. 3, 4, 6). The high degree of overlap between the successive chambers and the negligible growth rate acceleration for the final chamber found in *Velapertina* (Fig. 3A,B,E,F) indicate that this form achieved its terminal spherical shell morphology by

https://doi.org/10.1017/pab.2022.48 Published online by Cambridge University Press

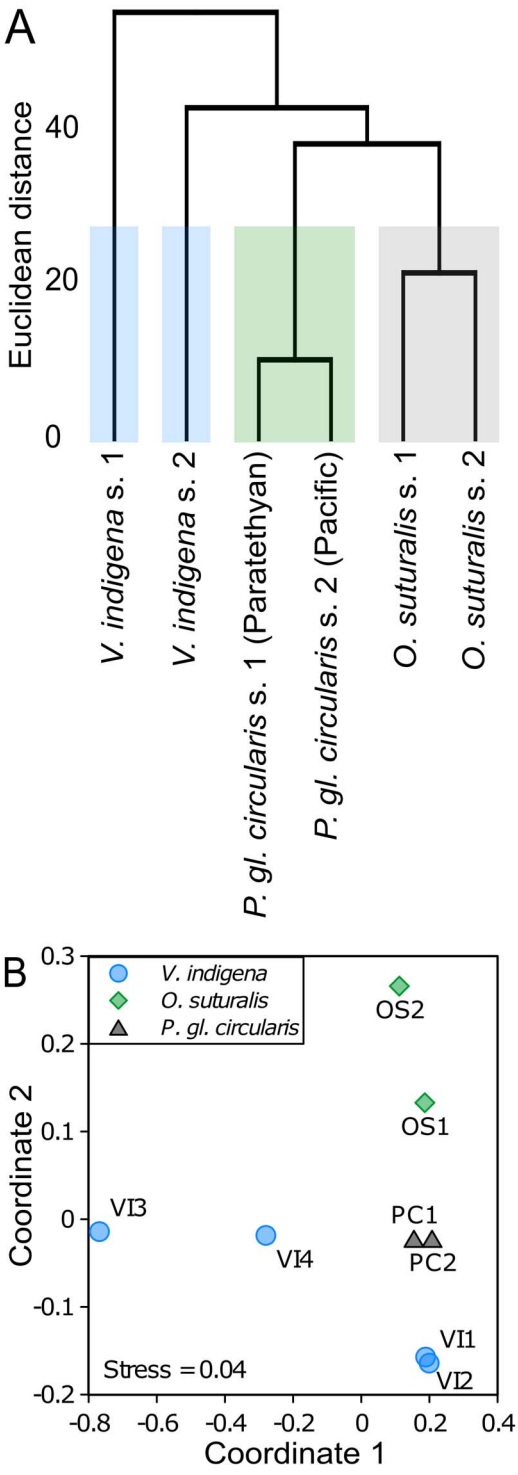

FIGURE 4. Cluster analysis (based on Euclidean distance and paired group clustering algorithm) of 11 variables describing shell coiling and architecture of two specimens of each of the three analyzed species (A) and a nonmetric multidimensional scaling (based on Euclidean distance) visualization of morphospace occupation including two additional *Velapertina* specimens (B). The analysis in B is based on parameters describing the ontogeny of chamber and shell shape and volume expansion determined from X-ray computed tomography scanning data of the five chambers added before the final chamber. All analyzed variables are listed in Table 1. The analysis indicates that the convergent adult shape of *Velapertina indigena* is the result of a different ontogenetic sequence than in the *Praeorbulina–Orbulina* lineage.

progressively more overlapping chambers of similar size, whereas in *Orbulina*, the spherical shell emerges only in the final growth stage as a result of massive growth acceleration of the final chamber that envelops the entire shell (Fig. 6).

Indeed, next to the lack of growth acceleration, the final chamber in *Velapertina* is less globular (Fig. 3C,D) and does not completely encompass the earlier parts of the shell, as is the case in *Praeorbulina* and *Orbulina* (Figs. 2, 6). Instead, the analyzed individuals of *Velapertina* bear consistent differences in shell architecture before the development of the final chamber (Fig. 4), implying that their pre-adult morphology is not consistent with that of *Praeorbulina* and *Orbulina*. In other words, the final chamber is not required to differentiate between the two lineages, because *Velapertina* is characterized by more overlap between the successive chambers, with centroids localized closer to the coiling axis (R = 87.36), throughout the early ontogeny, whereas in *Praeorbulina–Orbulina*, the pre-adult part of the shell reveals a more loosely coiled and more evolute growth geometry with less overlap between successive chambers, occupying more whorls and with chamber centroids disposed far from the coiling axes (R = 121.28; Fig. 6). Thus, next to the Paleogene *Orbulinoides* (Cordey 1968), the Neogene *Orbulina* (d'Orbigny 1839), and *Globigerinatella* (Cushman and Stainforth 1945), *Velapertina* very likely represents the fourth example of the evolution of spherical shell shape among planktonic foraminifera. However, unlike the three other examples, in the case of *Velapertina*, the ancestor remains unclear. Sediment layers recording transitional forms leading to *Velapertina* have not yet been described, which likely indicates rapid

https://doi.org/10.1017/pab.2022.48 Published online by Cambridge University Press

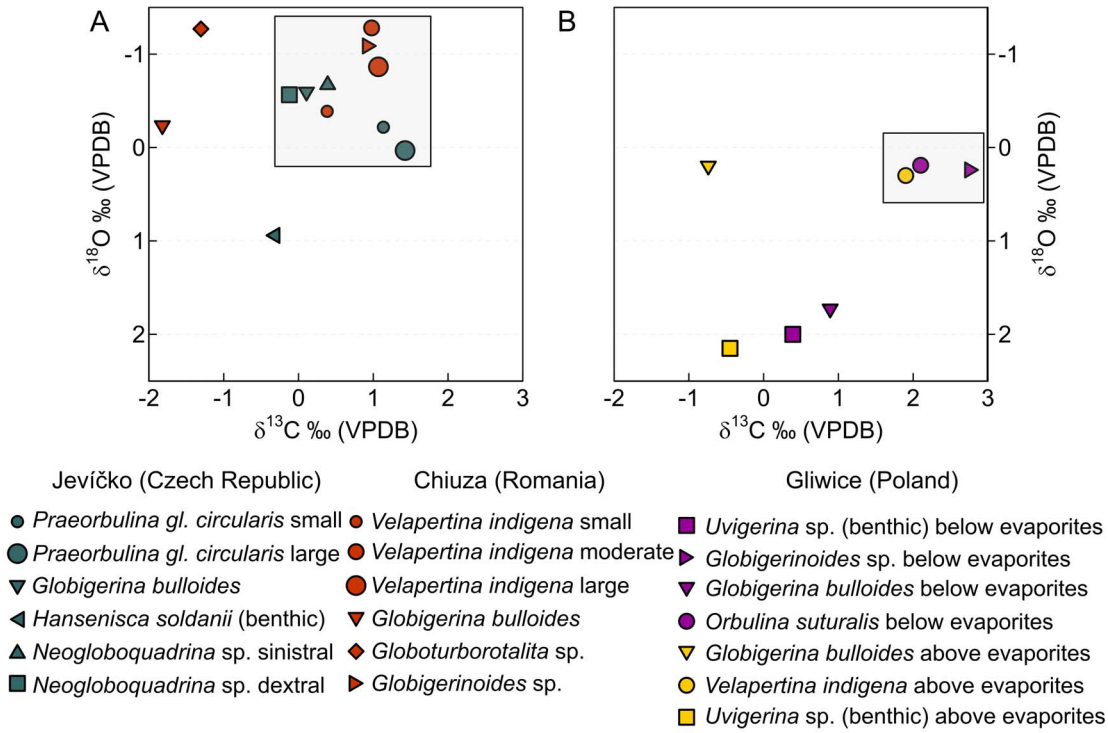

FIGURE 5. Habitat reconstruction of *Velapertina* relative to other planktonic foraminifera species based on $\delta^{13}C$ and $\delta^{18}O$ isotopes from (A) new measurements and (B) data from Durakiewicz et al. (1997).

speciation within a geographically limited population, akin to the concept of punctuated equilibria (Gould and Eldredge 1977, 1993). On the other hand, the ancestor ought to be sourced from within the globigerinid taxa that were present in the Paratethys Sea before the emergence of *Velapertina*. Although the emergence of supplementary apertures in planktonic foraminifera also occurred in parallel many times (Wade et al. 2018), it appears more parsimonious to speculate that this trait would have already been present in the ancestor, as was the case in the emergence of the *Orbulina* lineage (Blow 1956; Jenkins 1968; Pearson et al. 1997). This would imply an ancestry of *Velapertina* in either the *Trilobatus* or *Globigerinoides* lineages, which were both present in the Paratethys and possess supplementary apertures. In our opinion, there is no way to pinpoint the ancestor any closer at this time, because the only remaining character, shell wall texture, is inconclusive. Therefore, in the absence of knowledge of the exact ancestor of *Velapertina*, we retain the classification of the lineage in a separate genus.

The existence of a fourth independent case of the evolution of spherical shell shape in planktonic foraminifera, in *Velapertina*, allows us to assess the degree of developmental integration during the emergence of this character. When evolution is directed toward spherical shell geometry, the foraminifera are "faced" with the problem of retaining communication with the exterior through an aperture without compromising the spherical shape. The morphological transitions in *Orbulinoides*, *Orbulina*, and *Globigerinatella* exhibit a trend, where from a certain point along the transition toward a spherical shell, the large primary aperture transforms into a series of small sutural apertures. Remarkably, the same is observed in *Velapertina*, indicating that this may be the only solution available because of constructional constraints (Raup 1966) during the morphogenesis of subsequent chambers. In *Orbulina* and *Globigerinatella*, where the terminal chamber encompasses the

https://doi.org/10.1017/pab.2022.48 Published online by Cambridge University Press

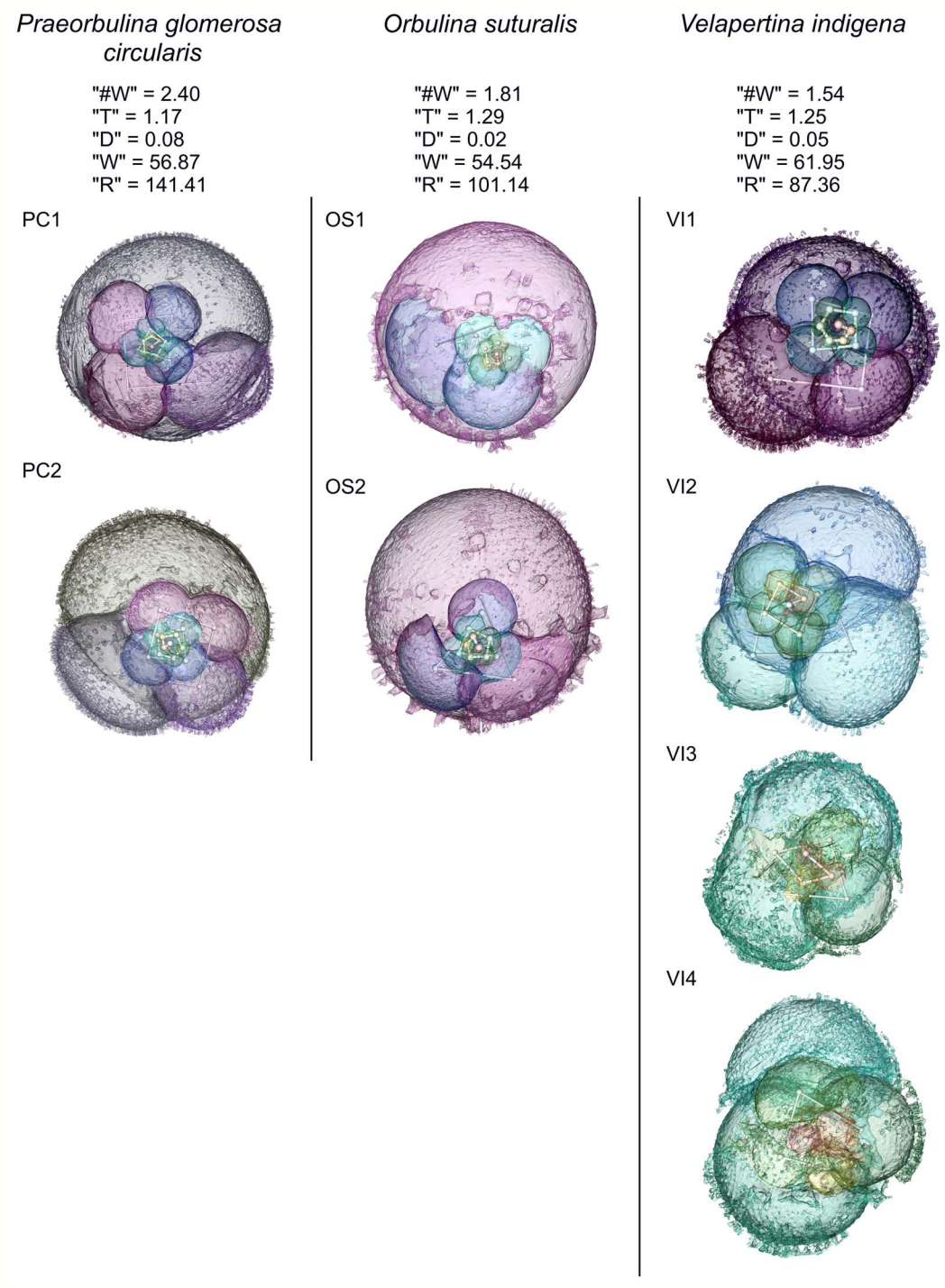

FIGURE 6. X-ray computed tomography scanning reconstructions visualizing the shell ontogeny of all analyzed specimens by holding the external shell transparent. Specimens are labeled as in Fig. 4B. The successive positions of chamber centroids are shown in the top row specimens to visualize the shape of the logarithmic spiral from which the Raupian parameters shown next to the analyzed specimens have been extracted. This comparison show that the *Velapertina* has more overlapping chambers of similar size with chamber centroids disposed near to the coiling axes, whereas in *Praeorbulina* and *Orbulina*, the coiling is more evolute with a lower degree of overlap between the successive chambers that occupy more whorls and are disposed far from the coiling axes. The Raupian parameters of the logarithmic spiral (Raup 1966) are provided for each specimen.

https://doi.org/10.1017/pab.2022.48 Published online by Cambridge University Press

entire shell, this sequence progressed further, whereby next to the sutural apertures multiple areal apertures appeared throughout the final chamber (Blow 1956). The Paratethyan *Velapertina* appears to have followed the same path of transformation; because the terminal chamber is not completely encompassing, there are still many sutural apertures, but it also possessed the first clearly identifiable areal apertures appearing in the final chamber (Popescu 1976; see also Fig. 2). This indicates a consistent connection between shell architecture and aperture types during the evolution of a spherical shell, with the emergence of areal apertures as the prerequisite for maintaining the trophic behavior of the evolving lineage while possessing a spherical shell shape.

The independent origin of spherical shells in *V. indigena* implies that the similar morphological traits of *Velapertina* and *Orbulina* are the result of parallel evolution, a common phenomenon in the history of planktonic foraminifera (Norris 1991; Coxall et al. 2007; Weiner et al. 2015). Coxall et al. (2007) documented the emergence of digitate chambers and concluded that there must have been an environmental driver associated with life in a deeper environment that favored this chamber morphology. Our stable isotopic analysis of *V. indigena* indicates essentially the same habitat and presence of symbionts as in the coexisting *Orbulina* lineage and the likely ancestral *Globigerinoides* or *Trilobatus* (Pearson et al. 1997; Fig. 5). This in line with previous observations reporting no depth parapatry in the evolution of *Orbulina* (Pearson et al. 1997) and implies that the emergence of the spherical shell shape was not associated with a change in depth habitat. On the other hand, the independent evolution of the same trait in a coexisting lineage in the Central Paratethys indicates that there likely was a strong functional advantage of this shape at that time. This prompts the question of why the spherical shell shape is so advantageous for planktonic foraminifera? As already recognized by Pearson et al. (1997), a spherical shell shape creates the minimum possible surface-to-volume ratio. Surface-to-volume ratio is an important parameter for cell physiology, determining the rate of key processes like gas exchange. Minimizing this ratio implies a lifestyle where gas exchange is not limiting (no oxygen depletion; Burke et al. 2018), and its potential advantage could be that the spherical shell shape requires the least amount of material to achieve the maximum volume.

Having established that *Velapertina* evolved independently from *Orbulina*, it also has to be accepted that this peculiar form was endemic throughout its existence to the semi-isolated system of partly interconnected basins of the Central Paratethys (Fig. 1). The middle Miocene planktonic foraminifera composition in this complex marine realm was affected by tectonics and sea-level changes, creating marine gateways that facilitated population exchange between the Mediterranean and the Paratethys. The most prominent gateway during the Langhian was the Trans-Tethyan Trench Corridor, east of the Alps, which remained open until the Serravallian (Rögl 1998; Kováč et al. 2007, 2017; Fig. 1). The timing of its restriction appears to coincide with the emergence of *Velapertina*, and because *Velapertina* has never been reported outside the Central Paratethys, the speciation of *Velapertina* likely took place in the then semi-isolated Central Paratethys. Here, the species clearly evolved in the presence of the *Orbulina* lineage, with which it co-occurred throughout the Central Paratethys (Fig. 1) and with which it shared its habitat (Fig. 5). It is unclear from the stratigraphic resolution of our data if *V. indigena* evolved in the absence of *Orbulina* in some limited basins of the Paratethys, but certainly *Velapertina* co-occurred with *Orbulina* shortly after its emergence (Fig. 1). Assessing the spatial and temporal origin of *Velapertina* would require more detailed stratigraphic analysis of the basins where the co-occurrence of the two lineages is documented. However, likely because of the restricted connection of the Central Paratethys in the Serravallian, the endemic *Velapertina* never succeeded in invading the world ocean or the Mediterranean. Like all other planktonic foraminifera inhabiting the Paratethyan basins, it fell victim to the ongoing environmental transformation due to further restriction of the Central Paratethys, culminating in the Tortonian with the Pannonian Lake (Kováč et al. 2007, 2017).

The isolated nature of the Paratethys, and frequent changes in the regional paleogeography

https://doi.org/10.1017/pab.2022.48 Published online by Cambridge University Press

(Fig. 1) very likely affected the nature of the regional water-column stratification. We note that changes in stratification have been considered important drivers of size disparity (Schmidt et al. 2004) as well as diversity (Lowery et al. 2020) of planktonic foraminifera, and we speculate that it may have been this aspect of the regional environment that led to the emergence as well as the extinction of *Velapertina*.

As a result of its peculiar biogeography, *Velapertina* is one of only a few species of planktonic foraminifera with a known place of origin and an endemic distribution. Unlike the bipolar or Indopacific–Atlantic isolation known for some cryptic (Darling et al. 2003, 2007; Morard et al. 2011, 2019; Quillévéré et al. 2013; Weiner et al. 2015) or even morphologically distinguishable species (Lazarus et al. 1995; Kučera and Kennett 2000), the distribution area of *Velapertina* was strikingly small and restricted. It is possible that this unusual degree of restriction facilitated speciation among the enclosed foraminifera, as evidenced by the existence of other endemic species that appear restricted to the Paratethys (Rögl 1994).

Conclusions

The evolution of the spherical shell shape of *Orbulina universa* is a textbook example of the emergence of a complex character documented by a series of transitional steps, combining chamber growth rate and aperture modifications. Here we show that shortly after the emergence of *Orbulina*, the enigmatic lineage of *Velapertina* from the Central Paratethys iterated the same steps of morphological integrations toward spherical shell shape. Through detailed X-ray computed tomography scanning analyses of *Praeorbulina glomerosa circularis*, *Orbulina suturalis*, and *Velapertina indigena*, we revealed a consistent difference in the adult and pre-adult growth patterns of the two lineages, indicating that the *Velapertina* lineage had a different origin. This indicates that the final spherical morphology with areal apertures in *V. indigena* results from parallel evolution with the *Orbulina* lineage. Because of increasing restriction of the biogeographic province, *Velapertina* remained endemic to the Paratethys throughout its short existence. The fact that it evolved shortly after *Orbulina* and shared the same habitat indicates a common environmental driver favoring spherical shells in planktonic foraminifera, implying that this complex character evolved in response to a specific environmental stimulus, such as the emergence of a specific habitat.

Acknowledgments

We would like to thank the editor and two anonymous reviewers for their constructive comments on earlier versions of this article. We thank K. Holcová for valuable discussions, M. J. Sabo for proofreading the manuscript, and S. Filipescu for providing material from Chiuza (Romania). The present study used a sample obtained during the Ocean Drilling Program (Leg 144). P.K. was supported by the Collegium Talentum Programme of Hungary, the Slovak Research and Development Agency under the contracts APVV-20-0079 and APVV 17-0555, the Grants for Young Scientists of the Comenius University in Bratislava (UK/214/2019), the German Academic Exchange Service (DAAD) Research Grant for Doctoral Candidates and Young Academic Scientists, the German Academic Exchange Service (DAAD) STIBET Scholarship, the National Scholarship Programme of the Slovak Republic, and the Erasmus+ Programme of the European Commission. We also acknowledge funding through the Cluster of Excellence "The Ocean Floor—Earth's Uncharted Interface."

Declaration of Competing Interests

The authors declare no competing interests.

Data Availability Statement

Supplementary Table 1 is available from the Dryad Digital Repository: https://doi.org/10.5061/dryad.7d7wm37zr. Planktonic foraminifera data and the X-ray computed tomography scanning data are available online at PANGAEA Data Publisher: https://doi.org/10.1594/PANGAEA.952343.

Literature Cited

Aurahs, R., G. W. Grimm, V. Hemleben, C. Hemleben, and M. Kučera. 2009. Geographical distribution of cryptic genetic

https://doi.org/10.1017/pab.2022.48 Published online by Cambridge University Press

types in the planktonic foraminifer *Globigerinoides ruber*. Molecular Ecology 18:1692–1706.

Báldi, K. 2006. Paleoceanography and climate of the Badenian (Middle Miocene, 16.4–13.0 Ma) in the Central Paratethys based on foraminifera and stable isotope ($\delta^{18}O$ and $\delta^{13}C$) evidence. International Journal of Earth Science (Geologische Rundschau) 95:119–142.

Baum, D., and J. Titschack. 2016. Cavity and pore segmentation in 3D images with ambient occlusion. Pp. 113–117 *in* Proceedings of the 18th EG/VGTC Conference on Visualization. Groningen, Netherlands.

Bicknell, R. D. C., K. S. Collins, M. Crundwell, M. Hannah, J. S. Crampton, and N. E. Campione. 2018. Evolutionary transition in the late Neogene planktonic foraminiferal genus *Truncorotalia*. iScience 8:295–303.

Birch, H., H. K. Coxall, P. N. Pearson, D. Kroon, and M. O'Regan. 2013. Planktonic foraminifera stable isotopes and water column structure: disentangling ecological signals. Marine Micropaleontology 101:127–145.

Blow, W. H. 1956. Origin and evolution of the foraminiferal genus *Orbulina* d'Orbigny. Micropaleontology 2:57–70.

Brummer, G.-J. A., C. Hemleben, and M. Spindler. 1987. Ontogeny of extant spinose planktonic foraminifera (*Globigerinidae*): a concept exemplified by *Globigerinoides sacculifer* (Brady) and *G. ruber* (d'Orbigny). Marine Micropaleontology 12:357–381.

Bubík, M. 2015. Tracking Richard Johann Schubert in Moravia: field-trip guide. Pp. 88–97 *in* M. Bubík, A. Ciurej, and M. A. Kaminski, eds. 16th Czech-Slovak-Polish Palaeontological Conference & 10th Polish Micropalaeontological Workshop, Abstracts Book and Excursion Guide. Grzybowski Foundation & Micropress Europe, Kraków–New York.

Burke, J. E., W. Renema, M. J. Henehan, L. E. Elder, C. V. Davis, A. E. Maas, G. L. Foster, R. Schiebel, and P. M. Hull. 2018. Factors influencing test porosity in planktonic foraminifera. Biogeosciences 15:6607–6619.

Caromel, A. G. M., D. N. Schmidt, and E. J. Rayfield. 2017. Ontogenetic constraints on foraminiferal test construction. Evolution and Development 19:157168.

Cordey, W. G. 1968. Morphology and phylogeny of *Orbulinoides beckmanni* (Saito, 1962). Palaeontology 11:371–375.

Coxall, H. K., P. A. Wilson, P. N. Pearson, and P. F. Sexton. 2007. Iterative evolution of digitate planktonic foraminifera. Paleobiology 33:495–516.

Cushman, J. A., and R. M. Stainforth. 1945. The foraminifera of the Cipero Marl Formation of Trinidad, British West Indies. Cushman Laboratory for Foraminiferal Research, Special Publication 14:1–75.

Darling, K., M. Kučera, C. M. Wade, P. von Langen, and D. Pak. 2003. Seasonal distribution of genetic types of planktonic foraminifer morphospecies in the Santa Barbara Channel and its paleoceanographic implications. Paleoceanography 18:1032.

Darling, K., M. Kučera, and C. M. Wade. 2007. Global molecular phylogeography reveals persistent Arctic circumpolar isolation in a marine planktonic protist. Proceedings of the National Academy of Sciences USA 104:5002–5007.

Darwin, C. R. 1859. On the origin of species by means of natural selection; or, The preservation of favoured races in the struggle for life. John Murray, London.

Decima, P. F., and H. M. Bolli. 1970. Evolution and variability of *Orbulinoides beckmanni* (Saito). Eclogae Geologicae Helvetiae 62:883–905.

d'Orbigny, A. 1839. Foraminifères. Pp. 1–224 *in* M. R. de la Sagra, ed. Histoire physique et naturelle de l'Ile de Cuba. Arthus Bertrand, Paris.

Durakiewicz, T., M. Gonera, and D. Peryt. 1997. Oxygen and carbon isotopic changes in the middle Miocene (Badenian) foraminifera of the Gliwice area (SW Poland). Bulletin of the Polish Academy of Sciences, Earth Sciences 45:145–155.

Ezard, T. H. G., K. M. Edgar, and P. M. Hull. 2015. Environmental and biological controls on size-specific $\delta^{13}C$ and $\delta^{18}O$ in recent planktonic foraminifera. Paleoceanography 30:151–173.

Filipescu, S. 1996. Stratigraphy of the Neogene from the western border of the Transylvanian Basin. Studia Universitatis Babes-Bolyai, Geologia 41:3–78.

Gould, S. J., and N. Eldredge. 1977. Punctuated equilibria: the tempo and mode of evolution reconsidered. Paleobiology 3:115–151.

Gould, S. J., and N. Eldredge. 1993. Punctuated equilibrium comes of age. Nature 366:223–227.

Hohenegger, J., S. Ćorić, and M. Wagreich. 2014. Timing of the middle Miocene Badenian stage of the Central Paratethys. Geologica Carpathica 65:55–66.

Huber, B. T., M. R. Petrizzo, and K. G. MacLeod. 2020. Planktonic foraminiferal endemism at southern high latitudes following the terminal Cretaceous extinction. Journal of Foraminiferal Research 50:382–402.

Jenkins, D. G. 1968. Acceleration of the evolutionary rate in the *Orbulina* lineage. Contributions of the Cushman Foundation for Foraminiferal Research 29:133–140.

Kelley, P. H. 1983. Evolutionary patterns of eight Chesapeake group molluscs: evidence for the model of punctuated equilibria. Journal of Paleontology 57:581–598.

Kennett, J. P., and M. S. Srinivasan. 1983. Neogene planktonic foraminifera: a phylogenetic atlas. Hutchinson Ross, Stroudsburg, Penn.

Kováč, M., A. Andreyeva-Grigorovich, Z. Bajraktarević, R. Brzobohatý, S. Filipescu, L. Fodor, M. Harzhauser, N. Oszczypko, D. Pavelić, F. Rögl, B. Saftić, L. Sliva, and B. Studencka. 2007. Badenian evolution of the Central Paratethys Sea: paleogeography, climate and eustatic sea-level changes. Geologica Carpathica 58:579–606.

Kováč, M., N. Hudáčková, E. Halásová, M. Kováčová, K. Holcová, N. Oszczypko-Clowes, K. Báldi, G. Less, A. Nagymarosy, A. Ruman, T. Klučiar, and M. Jamrich. 2017. The Central Paratethys palaeoceanography: a water circulation model based on microfossil proxies, climate, and changes of depositional environment. Acta Geologica Slovaca 9:75–114.

Kováč, M., E. Halásová, N. Hudáčková, K. Holcová, M. Hyžný, M. Jamrich, and A. Ruman. 2018. Towards better correlation of the Central Paratethys regional time scale with the standard geological time scale of the Miocene Epoch. Geologica Carpathica 69:283–300.

Kováčová, P., L. Emmanuel, N. Hudáčková, and M. Renard. 2009. Central Paratethys paleoenvironment during the Badenian (middle Miocene): evidence from foraminifera and stable isotope ($\delta^{13}C$ and $\delta^{18}O$) study in the Vienna Basin (Slovakia). International Journal of Earth Sciences 98:1109–1127.

Kučera, M., and J. P. Kennett. 2000. Biochronology and evolutionary implications of late Neogene California margin planktonic foraminiferal events. Marine Micropaleontology 40:67–81.

Lazarus, D., H. Hilbrecht, C. Spencer-Cervato, and H. Thierstein. 1995. Sympatric speciation and phyletic change in *Globorotalia truncatulinoides*. Paleobiology 21:28–51.

Lirer, F., L. M. Foresi, S. M. Iaccarino, G. Salvatorini, E. Turco, C. Cosentino, F. J. Sierro, and A. Caruso. 2019. Mediterranean Neogene planktonic foraminifer biozonation and biochronology. Earth-Science Reviews 196:102869.

Lowery, C. M., P. R. Bown, A. J. Fraass, and P. M. Hull. 2020. Ecological response of plankton to environmental change: thresholds for extinction. Annual Review of Earth and Planetary Sciences 48:403–429.

Łuczkowska, E. 1955. Tortonian foraminifera from the Chodenice and Grabowiec Beds in the vicinity of Bochnia. Rocznik Polskiego Towarzystwa Geologicznego 23:77–190.

Łuczkowska, E. 1971. A new zone with *Praeorbulina indigena* (*Foraminiferida*, *Globigerinidae*) in the upper Badenian (Tortonian s.s.) of Central Paratethys. Annales de la Sociéte Géologique de Pologne 40:445–448.

https://doi.org/10.1017/pab.2022.48 Published online by Cambridge University Press

Malmgren, B. A., W. A. Berggren, and G. P. Lohmann. 1983. Evidence for punctuated gradualism in the late Neogene *Globorotalia tumida* lineage of planktonic foraminifera. Paleobiology 9:377–389.

Morard, R., F. Quillevere, C. J. Douady, C. de Vargas, T. de Garidel-Thoron, and G. Escarguel. 2011. Worldwide genotyping in the planktonic foraminifer *Globoconella inflata*: implications for life history and paleoceanography. PLoS ONE 6:e26665.

Morard, R., A. Fullberg, G. A. Brummer, M. Greco, L. Jonkers, A. Wizemann, A. K. M. Weiner, K. Darling, M. Siccha, R. Ledevin, H. Kitazato, T. de Garidel-Thoron, C. de Vargas, and M. Kučera. 2019. Genetic and morphological divergence in the warm-water planktonic foraminifera genus *Globigerinoides*. PLoS ONE 14:e0225246.

Müller, G. B., and G. P. Wagner. 1996. Homology, *Hox* genes, and developmental integration. American Zoologist 36:4–13.

Norris, R. D. 1991. Parallel evolution in the keel structure of planktonic foraminifera. Journal of Foraminiferal Research 21:319–331.

Olsson, R. K. 1964. *Praeorbulina* Olsson, a new foraminiferal genus. Journal of Paleontology 38:770–771.

Pearson, P. N. 1995. 2. Planktonic foraminifer biostratigraphy and the development of pelagic caps on guyots in the Marshall Islands Group. *In* J. A. Haggerty, S. Premoli, I. Rack, and M. K. McNutt, eds. Proceedings of the Ocean Drilling Program, Scientific Results, Vol. 144:21–59. Ocean Drilling Program, College Station, Tex.

Pearson, P. N., and T. H. G. Ezard. 2014. Evolution and speciation in the Eocene planktonic foraminifer *Turborotalia*. Paleobiology 40:130–143.

Pearson, P. N., N. J. Shackleton, and M. A. Hall. 1997. Stable isotopic evidence for the sympatric divergence of *Globigerinoides trilobus* and *Orbulina universa* (planktonic foraminifera). Journal of the Geological Society 154:295–302.

Pigliucci, M. 2003. Phenotypic integration: studying the ecology and evolution of complex phenotypes. Ecology Letters 6:265–272.

Popescu, G. 1969. Some new *Globigerina* (*Foraminifera*) from the Upper Tortonian of the Transylvanian Basin and the Subcarpathians. Revue Roumaine de Géologie, Géophysique et Géographie. Géologie 13:103–106.

Popescu, G. 1973. Contributions to the microbiostratigraphy of the middle Miocene from the Northern Transylvania. Studii şi cercetări de geologie, geofizică, geografie. Geologie 18:187–218.

Popescu, G. 1976. Phylogenetic remarks on the genera *Candorbulina*, *Velapertina* and *Orbulina*. Dări de Seamă ale Şedinţelor, Institutul de Geologie şi Geofizică 62:161–167.

Popescu, G. 1987. Marine middle Miocene microbiostratigraphical correlation in Central Paratethys. Dări de Seamă ale Şedinţelor, Institutul de Geologie şi Geofizică 72–73:149–167.

Quillévéré, F., R. Morard, G. Escarguel, C. J. Douady, Y. Ujiié, T. de Garidel-Thoron, and C. de Vargas. 2013. Global scale same-specimen morpho-genetic analysis of *Truncorotalia truncatulinoides*: a perspective on the morphological species concept in planktonic foraminifera. Palaeogeography, Palaeoclimatology, Palaeoecology 391:2–12.

Raup, D. M. 1966. Geometric analysis of shell coiling: general problems. Journal of Paleontology 40:1178–1190.

Reuss, E. A. 1854. Beitrage zur geognostischen Kenntniss Mährens. Jahrbuch der Kaiserlich-Königlichen Geologischen Reichsanstalt 5:657–765.

Rögl, F. 1994. *Globigerina ciperoensis* (*Foraminiferida*) in the Oligocene and Miocene of the Central Paratethys. Annalen des Naturhistorischen Museums in Wien 96A:133–159.

Rögl, F. 1998. Paleogeographic considerations for Mediterranean and Paratethys seaways (Oligocene to Miocene). Annalen des Naturhistorischen Museums in Wien 99A:279–310.

Scheiner, F., K. Holcová, R. Milovský, and H. Kuhnert. 2018. Temperature and isotopic composition of seawater in the epicontinental sea (Central Paratethys) during the middle Miocene Climate Transition based on Mg/Ca, $\delta^{18}O$ and $\delta^{13}C$ from foraminiferal tests. Palaeogeography, Palaeoclimatology, Palaeoecology 495:60–71.

Schmidt, D. N., S. Renaud, J. Bollmann, R. Schiebel, and H. R. Thierstein. 2004. Size distribution of Holocene planktic foraminifer assemblages: biogeography, ecology and adaptation. Marine Micropaleontology 50:319–338.

Spanbauer, T. L., S. C. Fritz, and P. A. Baker. 2018. Punctuated changes in the morphology of an endemic diatom from Lake Titicaca. Paleobiology 44:89–100.

Spezzaferri, S., M. Kučera, P. N. Pearson, B. S. Wade, S. Rappo, C. R. Poole, R. Morard, and C. Stalder. 2015. Fossil and genetic evidence for the polyphyletic nature of the planktonic foraminifera *Globigerinoides*, and description of the new genus *Trilobatus*. PLoS ONE 10:e0128108.

Stalling, D., M. Westerhoff, and H.-C. Hege. 2005. Amira—a highly interactive system for visual data analysis. Pp. 749–767 *in* C. D. Hansen and C. R. Johnson, eds. The visualization handbook. Butterworth-Heinemann, Burlington, Vt.

Szczechura, J. 1984. Morphologic variability in the *Globigerinoides-Orbulina* group from the middle Miocene of the Central Paratethys. Acta Palaeontologica Polonica 29:3–27.

Titschack, J., D. Baum, K. Matsuyama, K. Boos, C. Färber, W. A. Kahl, K. Ehrig, D. Meinel, C. Soriano, and S. R. Stock. 2018. Ambient occlusion—a powerful algorithm to segment shell and skeletal intrapores in computed tomography data. Computers and Geosciences 115:75–87.

Vlček, T., N. Hudáčková, M. Jamrich, E. Halásová, J. Franců, P. Nováková, M. Kováčová, and M. Kováč. 2020. Hydrocarbon potential of the Oligocene and Miocene sediments from the Modrany-1 and Modrany-2 wells (Danube Basin, Slovakia). Acta Geologica Slovaca 12:43–55.

Wade, B. S., P. N. Pearson, W. A. Berggren, and H. Pälike. 2011. Review and revision of Cenozoic tropical planktonic foraminiferal biostratigraphy and calibration to the geomagnetic polarity and astronomical time scale. Earth-Science Reviews 104:111–142.

Wade, B. S., R. K. Olsson, P. N. Pearson, B. T. Huber, and W. A. Berggren. 2018. Atlas of Oligocene planktonic foraminifera. Cushman Foundation for Foraminiferal Research Special Publication 46. Cushman Foundation for Foraminiferal Research, London.

Weiner, A. K. M., M. F. G. Weinkauf, A. Kurasawa, K. F. Darling, and M. Kučera. 2015. Genetic and morphometric evidence for parallel evolution of the *Globigerinella calida* morphotype. Marine Micropaleontology 114:19–35.

Westin, C. F., S. Peled, H. Gudbjartsson, R. Kikinis, and F. A. Jolesz. 1997. Geometrical diffusion measures for MRI from tensor basis analysis. P. 1742 *in* Proceedings of the 5th Annual Meeting of ISMRM. Vancouver, Canada.

https://doi.org/10.1017/pab.2022.48 Published online by Cambridge University Press